

ON INVERTING ASTEROSEISMIC DATA

Michael J. Thompson¹ and Jørgen Christensen-Dalsgaard²

¹Space & Atmospheric Physics, Blackett Laboratory, Imperial College, London, U.K

²Teoretisk Astrofysik Center, Danmarks Grundforskningsfond, and

Institut for Fysik og Astronomi, Aarhus Universitet, Århus, Denmark

ABSTRACT

Some issues of inverting asteroseismic frequency data are discussed, including the use of model calibration and linearized inversion. An illustrative inversion of artificial data for solar-type stars, using least-squares fitting of a small set of basis functions, is presented. A few details of kernel construction are also given.

Key words: Stars: structure – Stars: oscillations

1. INTRODUCTION

The accumulated experience in helioseismology of inverting mode frequency data provides a good starting point for asteroseismic inversion. In some rather superficial ways the circumstances of the two may seem very different: helioseismologists can use many more mode frequencies than will ever be possible for a more distant star, so that the resolution that can be achieved in helioseismic inversion is beyond the grasp of asteroseismology (an exception may be situations such as where modes are trapped in a narrow range of depth within the star). Another difference is that global parameters of the Sun such as its mass, radius and age are much better known than they are for other stars; hence the structure of the Sun is constrained *a priori* much more accurately than it is for a distant star, even if the input physics had been known precisely, which of course is not the case for the Sun or for other stars.

In more fundamental ways, though, helioseismic and asteroseismic inversion are much more similar than they are different. Helioseismology has not always been blessed with such a wealth of data, and helioseismologists in the early days of their subject learned the value of model calibration and asymptotic description (in particular of low-degree modes) for making inferences about the Sun. They also learned some of the dangers and limitations of drawing inferences from real data. The modal properties in many asteroseismic targets will be similar to the low-degree solar modes. Moreover, the principles of inversion are the same in both fields: obtaining localized information about the unseen stellar interior; assessing resolution; taking account of the effects of data errors; assessing what information the data really contain about the ob-

ject of study; judiciously adding additional constraints or assumptions in making inferences from the data.

This paper touches on a few of these points with regard to inverting asteroseismic data, including the usefulness of optimally localized averaging (OLA) kernels and model calibration using large and small frequency separations for solar-type oscillation spectra. Much more detail on those two topics can be found in the papers by Basu et al. (2001) and Monteiro et al. (2001), both in these proceedings.

The inversion problem predicates that one is able to perform first the forward problem. In the present context, that means the computation of the oscillation data (the mode frequencies) from the assumed structure of the star. Solving the forward problem always involves approximations or simplifying assumptions, because we cannot model the full complexities of a real star. The inverse procedure, inferring the structure (or dynamics) of the star from the observables, is ill-posed because, given one solution, there will almost invariably formally be an infinite number of solutions that fit the data equally well. The art of inverse theory is in no small part concerned with how to select from that infinity of possibilities. Actually, in various asteroseismic applications to date, e.g. to η Boo and certain δ Scuti stars, the problem is rather that one has so far been unable to find even a single solution that fits the data (see Christensen-Dalsgaard, Bedding & Kjeldsen 1995, Pamyatnykh et al. 1998). This may indicate that the some of the approximations made in the forward problem are inappropriate; it could also indicate that the errors in the data have been assessed incorrectly. In the present work, unless otherwise stated, we assume both that the forward problem can be solved correctly and that the statistical properties of the data errors are correctly known.

2. MODEL CALIBRATION

A relatively straightforward approach to the inverse problem is model calibration. At its conceptually simplest, this entails computing the observables for a set of models, possibly a sequence in which one or more physical parameters vary through a range of values, and choosing from among that set the one that best fit the data. ‘Best’ here is often taken to mean that model which minimizes the chi-squared value of a least-squares fit to the data. Given today’s fast computers, searches through large sets of models are feasible, either blindly or by using some search

algorithm such as genetic algorithm or Monte Carlo. Approaches similar to this have been undertaken for white dwarf pulsators (Metcalfe, Nather & Winget 2000; Metcalfe 2001) δ Scuti stars (Pamyatnykh et al. 1998), and pulsating sdB stars (Charpinet 2001). Depending on the way in which the method is applied, the resulting model may be constrained to be a member of the discrete set of calibration models, or could lie “between” them if interpolation in the set of models is permitted.

Model calibration is powerful and dangerous. It is powerful because it allows one to incorporate prejudice into the search for a solution and, suitably formulated, it can always find a best fit. It is dangerous for the same reasons: perhaps unwittingly on the part of the practitioner, it builds prejudice into the space of solutions that is considered. Also, even a satisfactory fit to the data does not mean that the solution model is necessarily like the real star: one can make a one-parameter model calibration to a single datum, but it is unclear what aspects of the resulting stellar model the datum is actually able to constrain. Examples of prejudice that model calibration may incorporate, for good or ill, are the choice of physics used to construct the models, and possible assumptions about the smoothness of the structure of the star. An insidious problem is that, if the approximations in the forward modelling introduce errors into the computed model observables, this can introduce a systematic error into the result of the model calibration. The Sun and solar-type stars provide a good example. Here the near-surface structure and the mode physics in that region are poorly modelled at present, and the simple approximations made introduce a systematic shift in the computed frequencies: low-frequency p modes have their upper turning point relatively deep in the star and are almost unaffected by the treatment of the surface layers, whereas modes of higher frequency have turning points closer to the surface and the error in their frequencies grows progressively bigger. In these circumstances, it is preferable not to calibrate to the frequency data themselves but rather to data combinations chosen to be relatively insensitive to the known deficiency in the forward modelling. In the near-surface layers, the eigenfunctions of solar p modes of low or intermediate degree l are essentially independent of l , so the error in the frequencies introduced by incorrectly modelling this region is just a function of frequency, scaled by the inverse of the mode inertia. This suggests that one should calibrate frequencies of solar-type stars to data combinations chosen to be insensitive to such an error.

Asymptotic analysis suggests other data combinations which can be used for model calibration and which are more discriminating than the raw frequency data. Monteiro et al. (2001) consider in some detail the use of the so-called large and small separations:

$$\Delta_{nl} = \nu_{n+1l} - \nu_{nl}, \quad \delta_{nl} = \nu_{nl} - \nu_{n-1l+2} \quad (1)$$

respectively. As Monteiro et al. demonstrate, the results of such a calibration, even for such global characteristics as

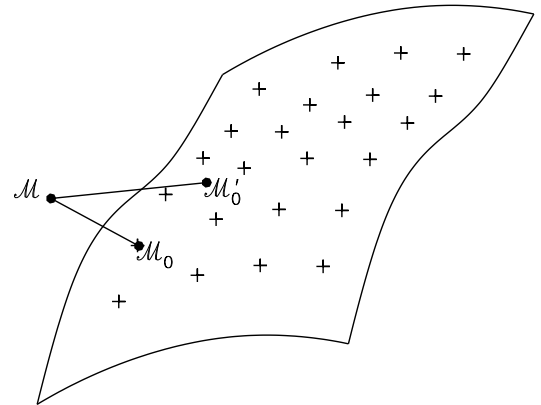


Figure 1. Model calibration selects a model M_0 in the space of models allowed by the calibration procedure: subsequent inversion using M_0 as reference determines a (hopefully improved) model M , not necessarily in the original space. If some other calibration selected a different model M'_0 , one hopes that the inversion procedure would bring one to the same or similar final model M .

the mass and age of the star, depend on the other physics assumed.

3. LINEARIZED INVERSION

Model calibration is just one approach to the inverse problem of inferring the stellar structure, which we may indicate schematically as \mathbf{X} , from the frequency data $\boldsymbol{\nu}$. How else may the nonlinear dependence $\boldsymbol{\nu} = \boldsymbol{\nu}(\mathbf{X})$ be inverted? A way which then allows application of a variety of techniques is to linearize about a reference model M_0 : inversion takes as input $\delta\boldsymbol{\nu}$, the difference between the observed data and the corresponding values that model M_0 predicts, and produces as output $\delta\mathbf{X}$, the estimated difference in structure between the star and M_0 . Since the structure of M_0 is known, the structure of the star can then be reconstructed. Of course, that is a naive hope, because of the inherent nonuniqueness discussed earlier, quite apart from issues of data errors. But one may at least produce a refinement on the initial model and indeed this new model can then be used as reference for a subsequent inversion as the next step of an iterative approach. Depending on the technique adopted, it is helpful and may be essential to have a reasonable starting guess in the form of the reference model M_0 . Model calibration using the large and small separations is a reasonable way to find such a model for solar-type stars.

Model calibration produces a solution \mathcal{M}_0 that is in the span (suitably defined) of the calibration set of models, illustrated schematically as a surface in Fig. 1. Inversion of the kind just described may then be used to proceed from \mathcal{M}_0 to a new model \mathcal{M} which may be ‘close’ to \mathcal{M}_0 but outside the span of the original calibration models. One hopes that the final model depends only weakly on the initial model, so that if by some other calibration (assuming different physics when calibrating the large and small separations, for example) one produces some other model \mathcal{M}'_0 , then the inversion step takes one close once more to the same final model \mathcal{M} .

One can imagine making all structural quantities in both the reference model and the target star dimensionless by taking out appropriate factors of the gravitational constant G and the stars’ masses M and radii R . Then the frequency differences $\delta\omega_{nl}$ between the same mode of order n and degree l in the two stars can be related to the differences in dimensionless structural quantities by an equation such as

$$\frac{\delta\omega_{nl}}{\omega_{nl}} = \delta \left(\ln \left(\frac{GM}{R^3} \right)^{\frac{1}{2}} \right) + \int_0^1 K_{u,Y}^{(nl)}(x) \frac{\delta u}{u}(x) dx + \int_0^1 K_{Y,u}^{(nl)}(x) \delta Y dx + \frac{F(\omega_{nl})}{E_{nl}} \quad (2)$$

where here the choice has been made to express the structural differences in terms of u , the ratio of pressure p to density ρ , and Y , the helium abundance by mass: for discussion of this choice, see Basu et al. (2001). Here, δu is the difference in dimensionless u between the two stars, the differences being evaluated at fixed fractional radius x in the star. The first term on the right-hand side is a constant and just reflects the $(GM/R^3)^{1/2}$ homologous dependence of the frequencies. The final term is some function of frequency, divided by mode inertia E_{nl} , which absorbs uncertainties from the near-surface layers. For some details of the construction of the kernel functions $K_{u,Y}^{(nl)}(x)$ and $K_{Y,u}^{(nl)}(x)$, which are known functions derivable from the reference model, see the Appendix. In an inversion, the left-hand side will be known; all terms on the right-hand side are to be inferred, including the difference in M/R^3 between the reference model and target star.

4. STRUCTURAL AND FREQUENCY DIFFERENCES

To motivate the rest of the paper we consider first the structural differences between a few stellar models. These will already indicate that rather small uncertainties in global parameters of stars, e.g. mass or age, can lead to large uncertainties in their structure. Of course the positive side of that is that the stellar structure is sensitive to those parameters and so, if the observable mode frequencies are in turn sensitive to those aspects of the structure then we may have some hope of using the observations to constrain e.g. the mass and age of the star rather precisely.

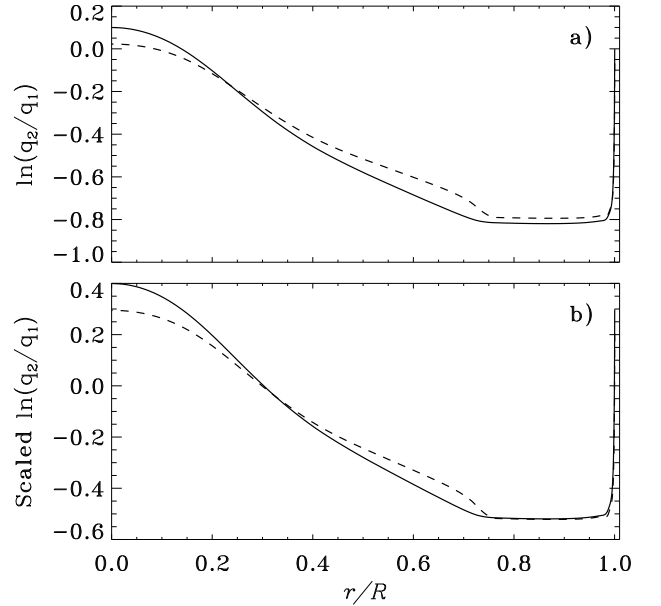


Figure 2. Relative differences in pressure p (solid curve) and density ρ (dashed curve), at fixed fractional radius, between ZAMS stars of mass $1.0M_\odot$ and $1.1M_\odot$ (in the sense $1.1M_\odot$ minus $1.0M_\odot$). (a) The quantities have not been homology-scaled before taking differences. (b) Quantities have been homology-scaled before differencing.

Panel (a) of Figure 2 shows the relative differences in pressure p and density ρ , at fixed fractional radius, between two ZAMS stars, of masses $1.0M_\odot$ and $1.1M_\odot$. We note that even for two stars with rather similar masses the differences are large, of order unity. Panel (b) shows the corresponding differences after the homology scaling has been taken out: this scaling is assumed taken out in the formulation presented in eq. (2). The effect is essentially to shift the two curves by a constant: although the differences are smaller, they are still large. These changes arise from nonhomologous differences in the surface layers which change the entropy of the convection zone. Indeed, writing $p = K\rho^{1+1/n}$ in the stars’ convective envelopes (in this context only, n denotes polytropic index), and noting that sound speed there is essentially determined by surface gravity, one finds that in that region

$$\delta \ln p \simeq \delta \ln \rho \simeq -n \delta \ln K. \quad (3)$$

Possibly of more direct relevance for inversion of eq. (2) is the difference in adiabatic sound speed c ($c^2 = \gamma_1 u$, where γ_1 is the first adiabatic exponent). As Fig. 3 shows, the relative differences in c^2 are smaller than the differences in pressure and density, but still quite substantial for stars that differ in mass by as little 10 per cent. Homology scaling has little effect on the differences in this case. For a reasonable range of masses, these differences scale linearly with the mass difference, so for example the cor-

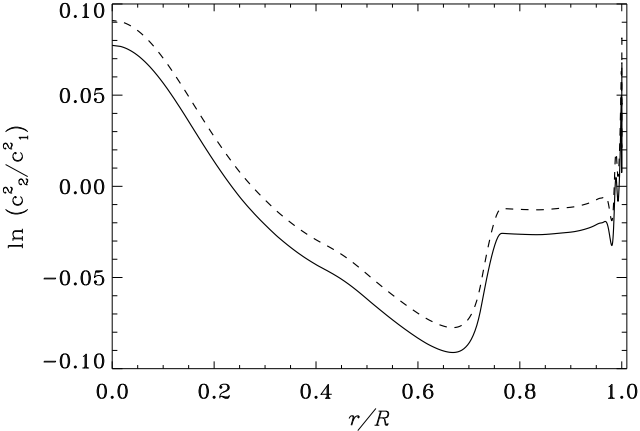


Figure 3. Relative differences in sound speed squared (c^2) at fixed fractional radius, between ZAMS stars of mass $1.0M_\odot$ and $1.1M_\odot$ (in the sense $1.1M_\odot$ minus $1.0M_\odot$): the two curves show unscaled (solid) and homology-scaled (dashed) differences.

responding scaled differences between $1.05M_\odot$ and $1.0M_\odot$ ZAMS stars are half those illustrated here, to a very good approximation.

5. INVERSION METHODS

A number of different linearized inversion methods have been developed in helioseismology, geophysics and diverse other areas of inversion applications. Two flexible approaches are Optimally Localized Averages (OLA) and Regularized Least Squares (see e.g. Christensen-Dalsgaard et al. 1990 for a description). The OLA method explicitly constructs a linear combination of kernels that is localized at some location in the star and is small elsewhere: the corresponding linear combination of relative frequency differences is then a measure of the localized average of the structural differences. The application of SOLA in the asteroseismology of solar-type stars is discussed and illustrated by Basu et al. (2001). We emphasize here that OLA reveals the true extent to which the seismic data alone can resolve the aspect of the stellar interior under study. Methods which on specific classes of problems appear to have superior performance to OLA in resolving aspects of the stellar interior are introducing nonseismic information or assumptions in addition to the frequency data.

The form of least-squares method used most extensively in helioseismology is regularized least-squares: the idea is to represent the solution with a set of basis functions more finely than can be resolved by the data and with ideally no bias about the form of the solution built into the basis; but then to minimize the sum of chi-squared fit to the data and a penalty term which is large if the solution has undesirable characteristics. The most used

penalty function is the integral over the star of the squared second derivative of the function under study with respect to radius.

A different way of regularizing the least-squares solution, without introducing a penalty term, is to choose a drastically smaller set of basis functions. This alternative, which we do not claim is intrinsically superior, may give apparently better results from few data if the basis functions are chosen with appropriate intuition or good fortune. The reason is that one can introduce a huge amount of prejudice into the solution by forcing it to have a form determined by the basis functions. Such a basis could, for example, force the buoyancy frequency to be zero in a convective core and permit a single discontinuity at the core boundary but not elsewhere: such assumptions may be reasonable, but it should be realized that they are additional to the seismic data. If the star actually had a second discontinuity, or a more gradual variation at the core boundary, such an inversion would not generally reveal those features. A helioseismic example is in finding the location of the base of the convective envelope, where remarkable precision ($0.001R_\odot$ taking into account uncertainties in abundance profiles, $0.0002R_\odot$ if the only uncertainty comes from data noise) has been claimed (Basu & Antia 1997): this is credible only insofar as the base of the convection zone has precisely the form assumed in the inversion, because the true resolution at that location is much coarser than that. The true resolution (e.g. vertically) is essentially limited by the reciprocal of the largest vertical wavenumber of the eigenfunctions corresponding to the available data (Thompson 1993).

6. AN EXPERIMENT WITH SPECIFIC BASIS FUNCTIONS

As a simple illustration of the apparent ability of least-squares inversion with a limited basis to infer structure even where the mode set has little resolving power, we take a basis of five functions chosen for algebraic convenience. They are approximately (but only approximately) able to represent the difference in u between ZAMS models of solar-like stars. The basis represents a function that is quadratic in $x \equiv r/R$ for $x < 0.1$ with zero derivative at $x = 0$, piecewise constant between radii $x = 0.1, 0.3$ and x_1 , quadratic between x_1 and x_2 and zero for $x > x_2$. The values of x_1 and x_2 , which are initially set to 0.65 and 0.75 respectively, are adjusted by hand to find a minimum of the chi-squared fit.

In the first of two illustrative applications, we consider the inversion of frequency data (65 modes: $l = 0$, $n = 14 - 32$; $l = 1$, $n = 13 - 29$, $l = 2$, $n = 15 - 30$, $l = 3$, $n = 16 - 28$) from a $1.05M_\odot$ ZAMS star. In a real application we would first calibrate the star by computing large and small separations from the data and using the approach of Monteiro et al. (2001) to arrive at a reference model; in fact we simply took a reference model which was a $1.0M_\odot$ ZAMS star. Before discussing the

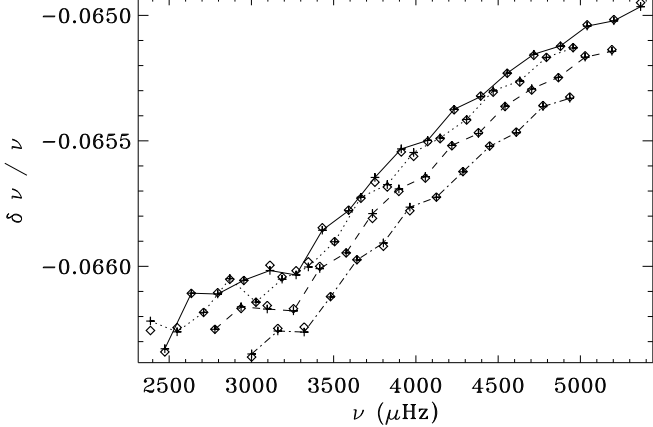


Figure 4. Relative frequency differences ($\nu = \omega/2\pi$ is cyclic frequency) between ZAMS stars of masses $1.0M_{\odot}$ and $1.05M_{\odot}$ (in the sense $1.05M_{\odot}$ minus $1.0M_{\odot}$). Lines join modes of the same degree: $l = 0$ (continuous line), $l = 1$ (dotted), $l = 2$ (dashed) and $l = 3$ (dot-dashed). Crosses indicate the actual values of the frequency differences, diamonds indicate the values produced by a least-squares fit of expression (2) using the basis functions discussed in Section 6. .

results of the inversion, we first consider the data, i.e. the relative frequency differences, shown in Fig. 4. (For clarity, no noise has been added to the data, though it was added for the inversions.) The dominant trends are that the values are negative, around -0.066 , because of the difference in M/R^3 between the two stars (in fact, $\delta \ln((GM/R^3)^{\frac{1}{2}}) = -0.0668$ for these two stellar models); and there is a roughly linear trend with frequency, in this frequency range, coming from near-surface differences. These two contributions can be estimated and removed by fitting an expression of the form (2): for illustration, we show in Fig. 5 what would remain: this is the signal from the interior, which contains the information that the inversion will use to infer conditions inside the star. The impression now is that the data contain a signal which has some oscillatory component (from the rather abrupt change in the structural differences at the base of the convective envelope) but is otherwise only weakly a function of frequency and increases with decreasing l , indicating that the more deeply penetrating (i.e. lower- l modes) sense $\delta u/u$ increasing in the deep interior as one gets closer to the centre of the star.

These features are indeed revealed by the inversion (Fig. 6), which compares the exact u -differences with the least-squares solutions for noise-free data and for data with Gaussian noise with zero mean and uniform standard deviations $\sigma = 0.1\mu\text{Hz}$, $0.2\mu\text{Hz}$, and $0.3\mu\text{Hz}$. The noise realization in the two panels is different, but within each panel the noise differs from case to case only by a

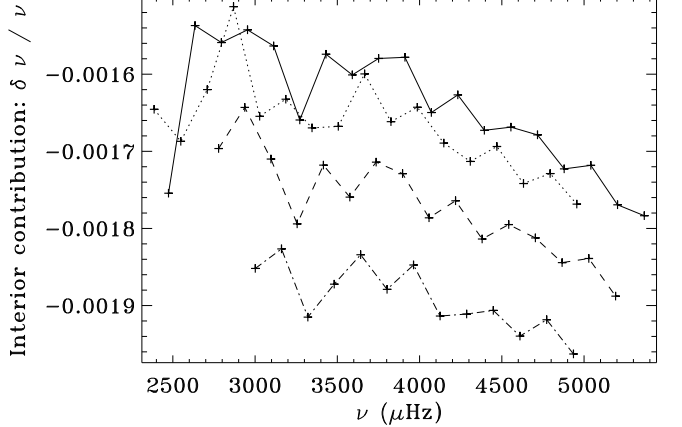


Figure 5. Residual frequency differences after the fitted constant term $\delta \ln(GM/R^3)^{\frac{1}{2}}$ and a two-term fit for the surface-like contribution $F(\omega)/E_{nl}$ have been removed. Line styles have the same meaning as in Fig. 4.

multiplicative scaling. It can be seen that for low noise levels this very small basis enables the differences to be recovered rather well, including the structure beneath the convection zone and the variation of δu in the core. For larger noise levels the artificiality of the basis functions becomes more apparent; also the solution for the higher noise levels is rather different for the two noise realizations, which gives some indication of the uncertainty even in this highly constrained solution.

A second example is an application to the same mode set but with data from model S_1 of Monteiro et al. (2001) and Gaussian data errors with $\sigma = 0.1\mu\text{Hz}$. This star is slightly more massive and more evolved than the Sun. Again, we omitted the calibration step and inverted relative to a reference model of the present-age Sun. The results are shown in Fig. 7. Again the qualitative behaviour of the differences is recovered reasonably, including the downturn in the core. The discrepancies are perhaps partly attributable to the fact that the basis functions are not so well suited for representing this case as the ZAMS case.

7. DISCUSSION

It is a prejudice of some stellar astrophysicists (it was indeed expressed a few times in Cordoba during the workshop) that helioseismic experience with the Sun provides a poor example when it comes to asteroseismic inversion. But the similarities between the two applications are much more significant than their differences. An extremely important aspect of inversion in any context is to assess what the data really tell you and what information is being introduced by other assumptions or constraints. OLA kernels (Basu et al. 2001) indicate what resolution can really be achieved without additional assumptions. But other

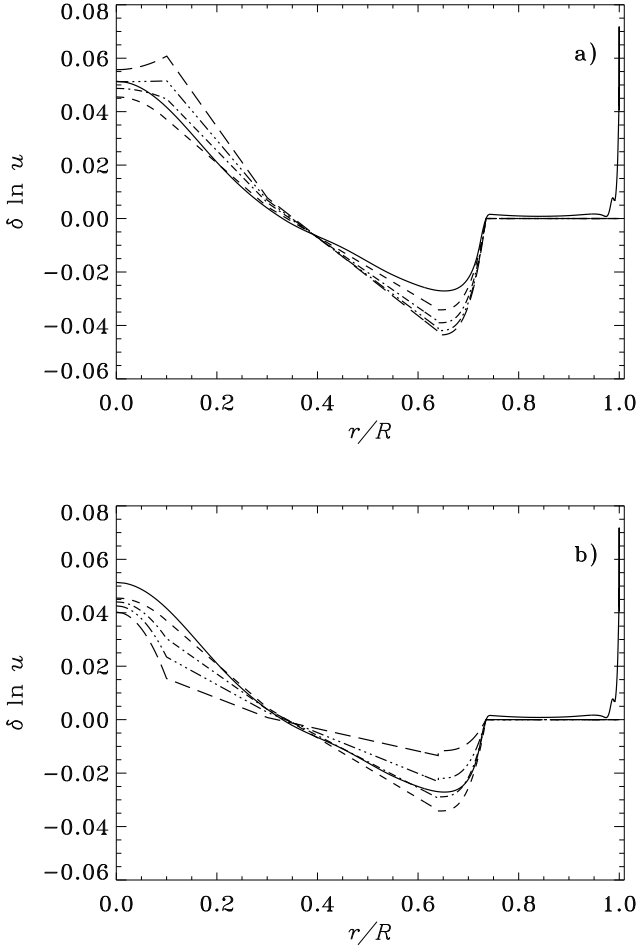


Figure 6. Inversion results for the relative difference in homology-scaled u between a $1.05M_{\odot}$ ZAMS star and a $1.0M_{\odot}$ ZAMS star. The solid curve shows the exact difference $\delta u/u$, and the short-dashed curve the solution from a least-squares inversion of noise-free data. The other curves show inversions of noisy data containing independent Gaussian errors with zero mean and uniform standard deviation $\sigma = 0.1 \mu\text{Hz}$ (dot-dashed), $\sigma = 0.2 \mu\text{Hz}$ (triple dot-dashed) and $\sigma = 0.3 \mu\text{Hz}$ (long-dashed). The upper and lower panel show two different realizations of the noise; within each panel the noise from one curve to another has just been scaled by a multiplicative factor.

approaches can advance our knowledge by allowing introduction of reasonable prejudices: e.g., looking for signatures of sharp features, or introducing specific basis functions. The best apparent results are likely to be achieved if those functions are physically motivated, because the solution will accord with our physical intuition (prejudice). This may of course be dangerous. Our example of a highly constrained least-squares inversion illustrates that qualitatively reasonable results can be obtained throughout a star by introducing assumptions about the form of the so-

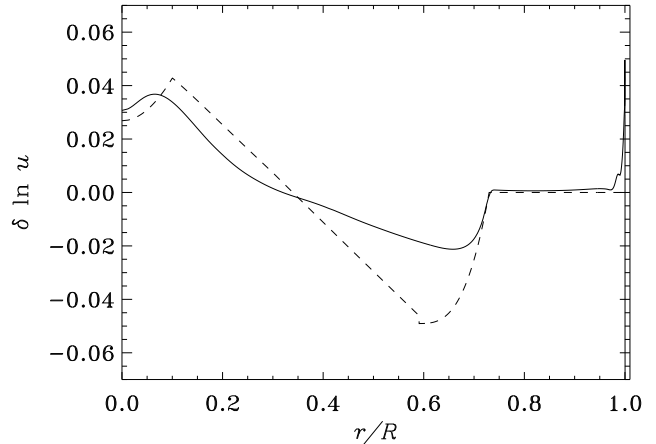


Figure 7. Inversion results for the relative difference in homology-scaled u between model S_1 of Monteiro et al. (2001) and a present-day standard solar model (in the sense S_1 minus solar model). The solid curve shows the exact differences, the dashed curve shows the solution of the least-squares fit to the data (which contained Gaussian noise with uniform standard deviation $0.1 \mu\text{Hz}$).

lution, even in regions where in fact the mode set provides little or no localized information (cf. Basu et al. 2001). One may have other grounds on which to believe that such a solution is plausible, but on the basis of the data alone it should be viewed sceptically.

Model calibration is a useful tool in its own right and for obtaining possible starting models for linearized asteroseismic inversions. Carefully used, model calibration allows one to build in some prejudice; and the combination of calibration and inversion extends the space of solutions that one explores.

Calibrating on large and small separations can be effective (Monteiro et al. 2001), always assuming that one has not neglected some important aspect of the physics: in that regard, the effects of rotation and magnetic fields need to be borne in mind (see Dziembowski & Goupil 1998), in solar-type stars as in many other pulsating stars.

Finally we note that mode identification may be a problem, even in solar-type stars. The asymptotic pattern of high-order p-mode frequencies may allow l to be determined, but there may be some uncertainty in n . Such an uncertainty can be allowed for in the inversion by adding to the right-hand side an extra term

$$G(\omega_{nl})/\omega_{nl} \quad (4)$$

where G is some function of frequency. We have verified that, with our ZAMS example, even restricting G to be a constant function removes quite satisfactorily the effect of a misidentification of n . More generally, G could judiciously be chosen to reflect the variation of the large separation with frequency.

ACKNOWLEDGEMENTS

This work was supported by the Danish National Research Foundation through the establishment of the Theoretical Astrophysics Center, and by the UK Particle Physics and Astronomy Research Council.

REFERENCES

- Basu, S., Antia, H. M., 1997, MNRAS, 287, 189
 Basu, S., Christensen-Dalsgaard, J., Thompson, M. J., 2001, these proceedings
 Charpinet, S., 2001, in Proc. IAU Colloq. 185, Radial and non-radial pulsations as probes of stellar physics, eds Aerts, C., Bedding, T. R. & Christensen-Dalsgaard, J., in press
 Christensen-Dalsgaard, J., Bedding, T. R., Kjeldsen, H., 1995, ApJ, 443, L29
 Christensen-Dalsgaard, J., Schou, J., Thompson, M. J., 1990, MNRAS, 242, 353
 Dziembowski, W. A., Goupil, M.-J., 1998, in Proc. "Workshop on Science with a Small Space telescope", eds Kjeldsen H. & Bedding T.R., Aarhus University, p. 69
 Gough, D. O., 1993, in Astrophysical fluid dynamics, Les Houches Session XLVII, eds Zahn, J.-P. & Zinn-Justin, J., Elsevier, Amsterdam, p. 399
 Gough, D. O., Thompson, M. J., 1991, in Solar interior and atmosphere, eds Cox, A. N., Livingston, W. C. & Matthews, M., Space Science Series, University of Arizona Press, p. 519
 Kosovichev, A. G., 1999, Journal of Computational and Applied Mathematics, 109, 1
 Metcalfe, T. S., 2001, Computational asteroseismology, Ph.D. thesis, University of Texas at Austin, USA
 Metcalfe, T. S., Nather, R. E., Winget, D. E., 2000, ApJ, 545, 974
 Monteiro, M. J. P. F. G., Christensen-Dalsgaard, J., Thompson, M. J., 2001, these proceedings
 Pamyatnykh, A. A., Dziembowski, W. A., Handler, G., Pikall, H., 1998, A&A, 333, 141
 Thompson, M. J., 1993, in Proc. GONG 1992: Seismic investigation of the Sun and stars, ed. Brown, T. M., ASP Conference Series, San Francisco, vol. 42, 141

APPENDIX

The derivation of kernels relating the linearized differences in structure to the differences in frequency (cf. eq. 2) has been discussed by, e.g., Gough & Thompson (1991), Gough (1993), and Kosovichev (1999). As all those authors show, the kernels for either of the pairs of variables (c^2, ρ) or (γ_1, ρ) are quite straightforward to derive from the equations of linear adiabatic oscillations together with the linearized equation of hydrostatic support. Obtaining kernels for various other pairs, including the pair (u, Y) used in this paper, can be accomplished by first obtaining kernels for one of the other two pairs and then using the following piece of manipulation. It is sufficiently ubiquitous (occurring often when one wishes to transform from kernels for a pair including ρ to some other variable pair) that we write it rather generally.

Let $\psi(r)$ be a solution of

$$\left(\frac{\psi'}{r^2 \rho} \right)' + \frac{4\pi G \rho \psi}{r^2 p} = \left(\frac{F(r)}{r^2 \rho} \right)', \quad (5)$$

where prime denotes differentiation with respect to r (or x if everything – including r – is expressed in dimensionless variables), for a given function $F(r)$ (so ψ is a functional of F), with boundary conditions $\psi(0) = 0$ and $\psi(R) = 0$. Then, provided $\delta m(0) = 0$ and $\delta m(R) = 0$, where $m(r)$ is the mass interior to radius r , and letting $\langle \dots \rangle$ denote integration from $r = 0$ to $r = R$ ($x = 0$ to $x = 1$),

$$\left\langle F(r) \frac{\delta \rho}{\rho} \right\rangle \equiv \left\langle -p (\psi/p)' \frac{\delta u}{u} \right\rangle. \quad (6)$$

Note that $\delta m(0) = 0$ holds in general; and in our present application, we scale all structural quantities by G , M and R to make them dimensionless, so $\delta m(R) = 0$ is forced to be true. These two conditions also mean that $\langle 4\pi r^2 \delta \rho \rangle$ is zero, so any multiple of $4\pi r^2 \rho$ may be added to a kernel multiplying $\delta \rho / \rho$. Note that such an additional contribution to $F(r)$ makes no change to the right-hand side of eq. (5) and hence the contribution to ψ from such an addition is zero.

Obtaining kernels for Y additionally requires an assumption about the equation of state through γ_1 , since the oscillations do not know directly about the chemical abundances. In the following we write

$$\gamma_{,p} \equiv \left(\frac{\partial \ln \gamma_1}{\partial \ln p} \right)_{\rho,Y}, \text{ etc.}, \quad \gamma_{,Y} \equiv \left(\frac{\partial \ln \gamma_1}{\partial Y} \right)_{\rho,p}. \quad (7)$$

Then for convenience we record the following transformations:

$$(c^2, \rho) \rightarrow (u, \gamma_1)$$

$$K_{\gamma_1, u} \equiv K_{c^2, \rho}, \\ K_{u, \gamma_1} \equiv K_{c^2, \rho} - p \left(\frac{\psi}{p} \right)' \quad (8)$$

with $F \equiv K_{\rho, c^2}$;

$$(\gamma_1, \rho) \rightarrow (u, Y)$$

$$K_{Y, u} \equiv \gamma_{, Y} K_{\gamma_1, \rho}, \\ K_{u, Y} \equiv \gamma_{, p} K_{\gamma_1, \rho} - p \left(\frac{\psi}{p} \right)' \quad (9)$$

with $F \equiv (\gamma_{, p} + \gamma_{, \rho}) K_{\gamma_1, \rho} + K_{\rho, \gamma_1}$; and

$$(u, \gamma_1) \rightarrow (u, Y)$$

$$K_{Y, u} \equiv \gamma_{, Y} K_{\gamma_1, u}, \\ K_{u, Y} \equiv \gamma_{, p} K_{\gamma_1, u} + K_{u, \gamma} - p \left(\frac{\psi}{p} \right)' \quad (10)$$

with $F \equiv (\gamma_{, p} + \gamma_{, \rho}) K_{\gamma_1, u}$.